ADVANCED MATERIALS

Supporting Information

for *Adv. Mater.*, DOI: 10.1002/adma.201604464

Field Effect Enhanced Hydrogen Evolution Reaction of MoS_2 Nanosheets

Junhui Wang, Mengyu Yan, Kangning Zhao, Xiaobin Liao, Peiyao Wang, Xuelei Pan, Wei Yang, and Liqiang Mai**

Submitted to ADVANCED MATERIALS

Supporting Information

Field Effect Enhanced Hydrogen Evolution Reaction of MoS_2 Nanosheets

Junhui Wang[1], Mengyu Yan[1,], Kangning Zhao[1], Xiaobin Liao[1], Peiyao Wang[2], Xuelei Pan[1], Wei Yang[1], Liqiang Mai[1,*]*

Mr. J. H. Wang, Dr. M. Y. Yan, Mr. K. N. Zhao, Mr. X. B. Liao, Ms. P. Y. Wang, Mr. X. L. Pan, Mr. W. Yang; Prof. L. Q. Mai
[1]State Key Laboratory of Advanced Technology for Materials Synthesis and Processing, Wuhan University of Technology, Wuhan 430070, P.R. China, [2]Department of Mechanical and Aerospace Engineering, Monash University, Victoria 3800, Australia.

E-mail: ymymiles@whut.edu.cn; mlq518@whut.edu.cn

Electrochemical characterization

The linear sweep voltammetry (LCV) with the scan rate of 5 mV s^{-1} was carried out with an electrochemical workstation (Autolab PGSTAT 302N). The catalytic current and potential *vs.* RHE were respectively calculated from the LCV data. The efficient catalytic area of MoS_2 nanosheet is about 50 μm^2 and the reference potential of SCE is 0.2415 V. In the blank experiment, the exposed SiO_2 area is 50 μm^2. In the other two control experiments, the react area of Au and Pt filament are 100 and 21000 μm^2, respectively. The overpotentials with different gate voltages are calculated at the catalytic current of 100 mA cm^{-2}.

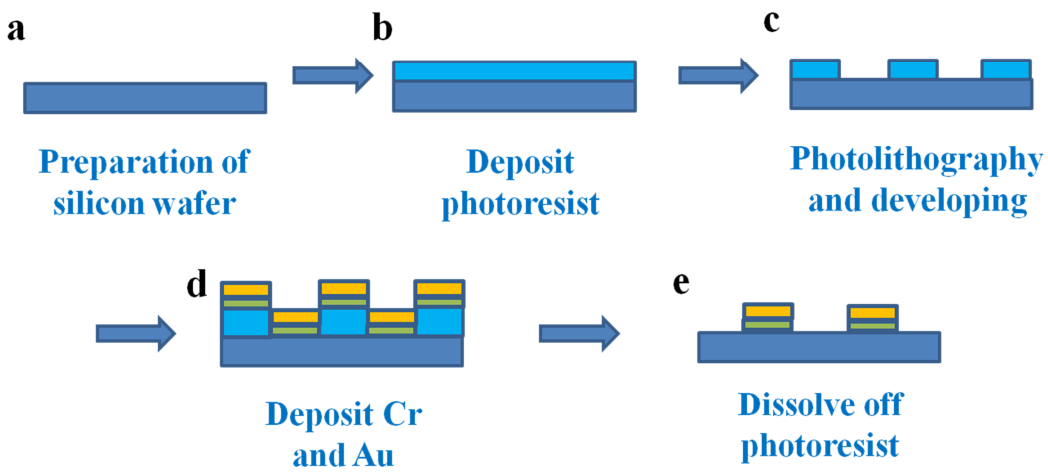

Figure S1. It mainly involves five steps during the fabrication process of the electrode. a) step 1, preparing a clean silicon wafers (with 300 nm SiO_2 layer) with the size of 2×1.5 cm^2. b) step 2, two layer photoresists are coated on the silicon wafer and baked on the hotplate. c) step 3, patterning the metal contacts pad with EBL/UV lithography, then developing and rinsing. d) step 4, Cr and Au layers with appropriate thickness are deposited by thermal evaporation. e) lifting-off the photoresist to expose the metal contacts pad.

The fabrication process of outer electrode and inner electrode are generally the same except the photoresist and photolithography technique. The LOL 2000/S1805 photoresists and ultraviolet lithography are used to fabrcate the outter electrode, while MMA/PMMA photoresists and electron beam lithography are used in fabrcating the inner electrode.

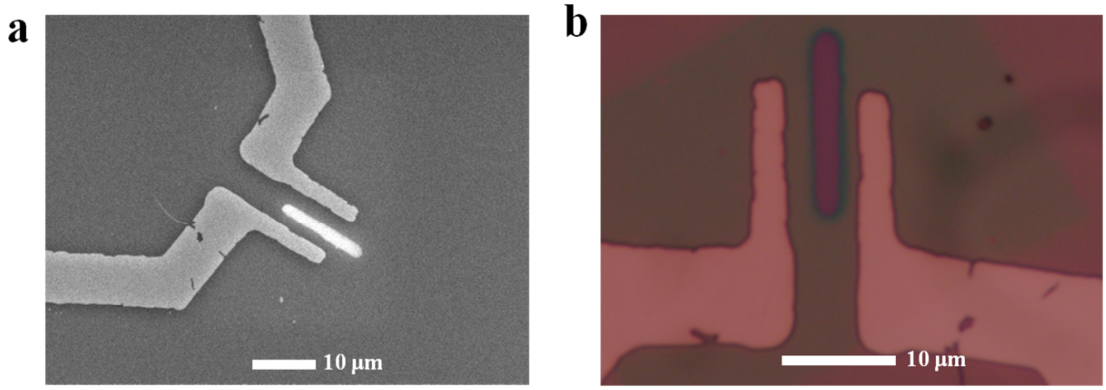

Figure S2. The SEM and optical images of the blank sample. In order to ensure the accuracy and reliability of experimental results, the fabrication processes and measurement means of the blank sample are fully the same with that of individual MoS_2 nanosheet based HER device.

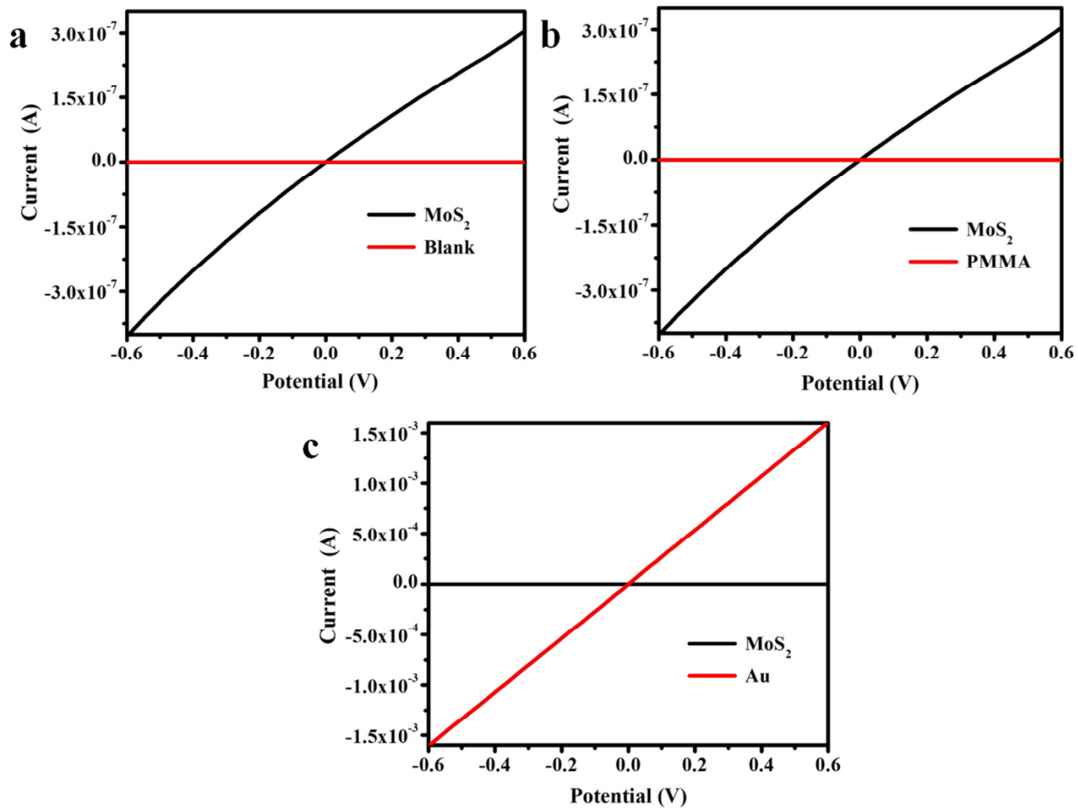

Figure S3. The respective *I-V* curves of a) blank sample and MoS_2. b) PMMA and MoS_2. c) Au and MoS_2. The conductances of blank sample and PMMA are far below than (more than 3 orders) that of MoS_2, which means the passivation layer is effectual and the leakage current can be neglectable. During the catalytic process, the resistance

of Au in the device can be ignored because the conductance of Au is 4 magnitudes larger than that of MoS_2.

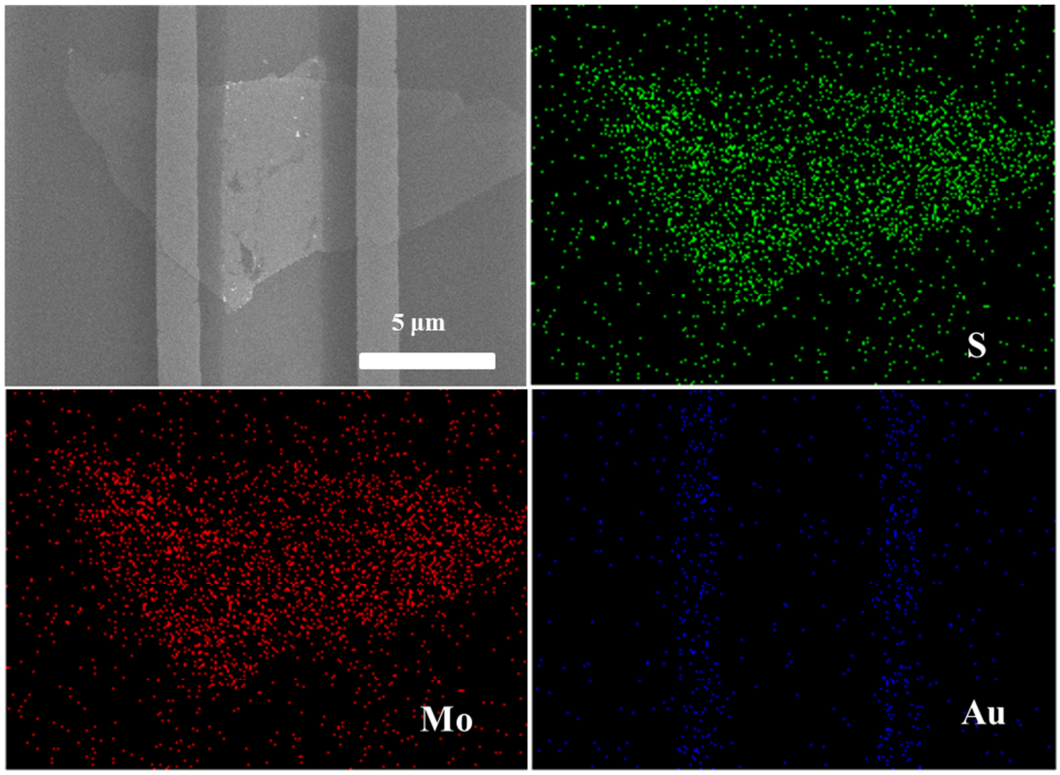

Figure S4. Energy dispersive spectrometry (EDS) element mapping images of MoS_2 nanosheet after catalytic measurement.

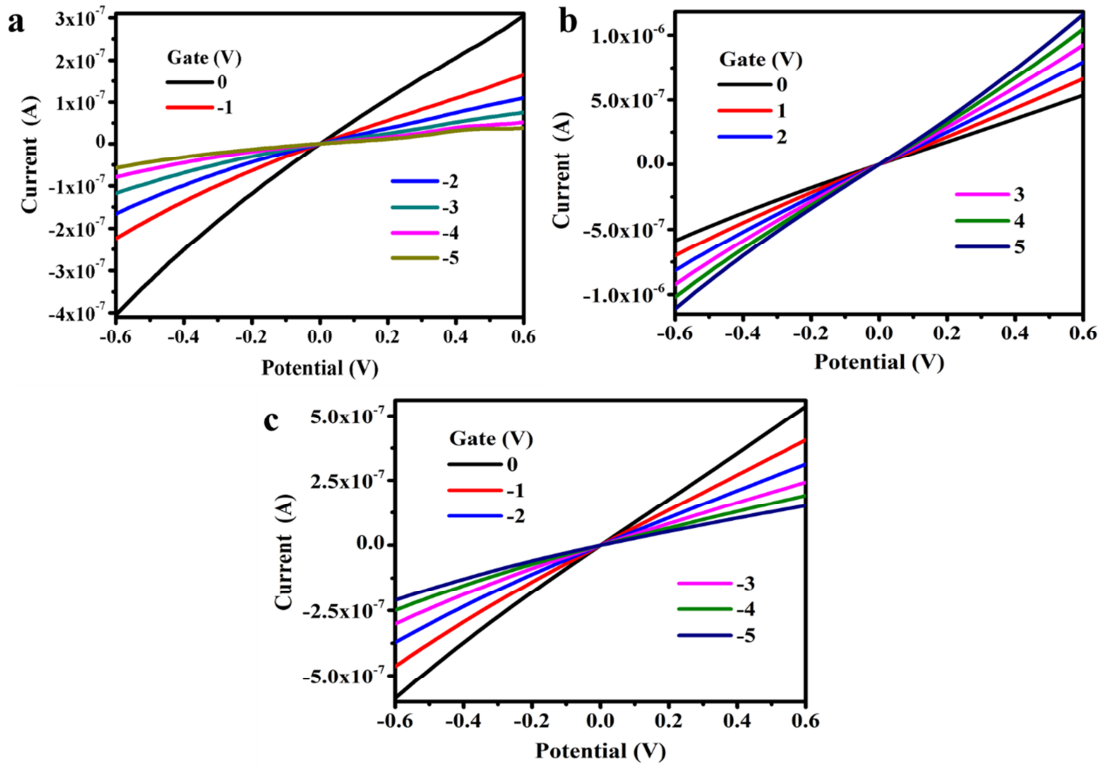

Figure S5. a) *I-V* curves of an individual MoS_2 nanosheet based HER device at different gate voltages. The gate voltages range from 0 to -5 V with the electrolyte. b-c) *I-V* curves of an individual MoS_2 nanosheet based HER device without electrolyte. The gate voltages range from 0 to 5 V (b) and 0 to -5 V (c).

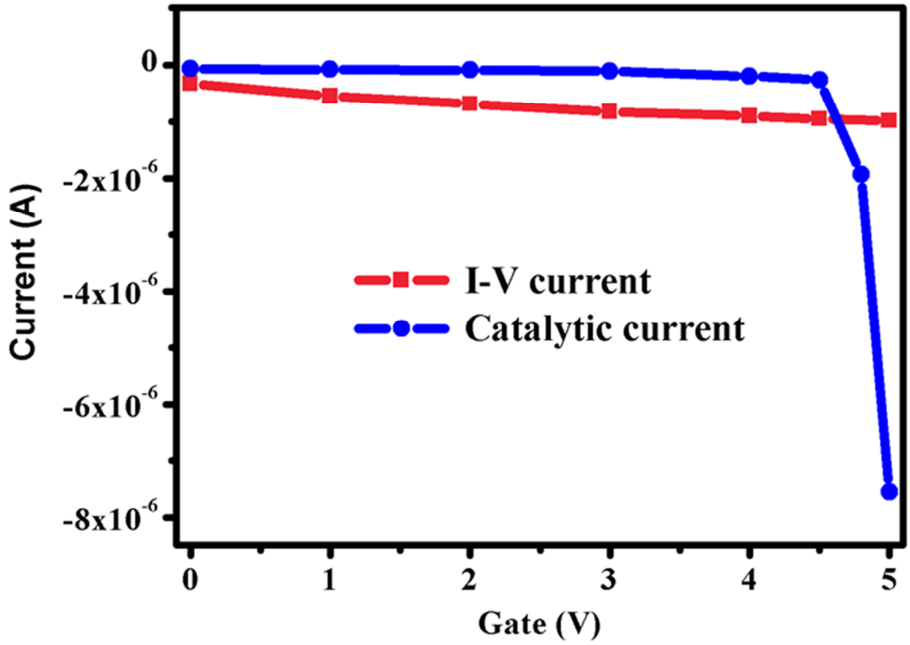

Figure S6. At the constant bias voltage of -0.5 V, the variation curve of the current in *I-V* curve and catalytic current with different gate voltages.

When the gate voltages range between 0 V and 4.5 V, the variations of the current in *I-V* curve and overall catalytic current respectively are 6.20E-7 A (from 3.25E-7 to 9.45E-7 A) and 1.98E-7 A (from 0.63E-7 to 2.61E-7 A). The absolute values of the current in *I-V* curve and its variation are both larger than that of overall catalytic current. These results reveal that the enhanced channel conductance is significant enough to improve the catalytic performance. However, the variation of catalytic current from gate of 4.5 to 5 V is tremendously large. The abnormal performance may come from the changes of control step in the overall catalytic reaction.

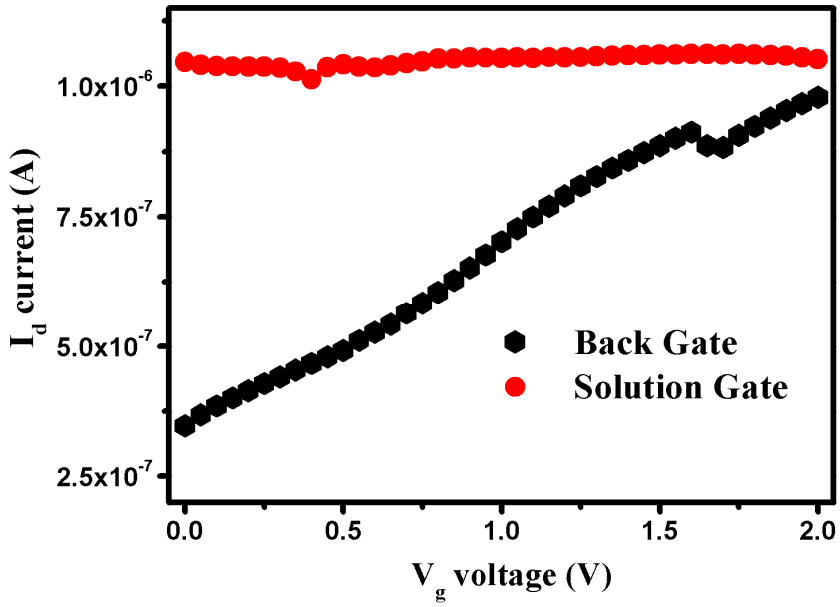

Figure S7. The I_d-V_g curve of the back gate and the solution gate.

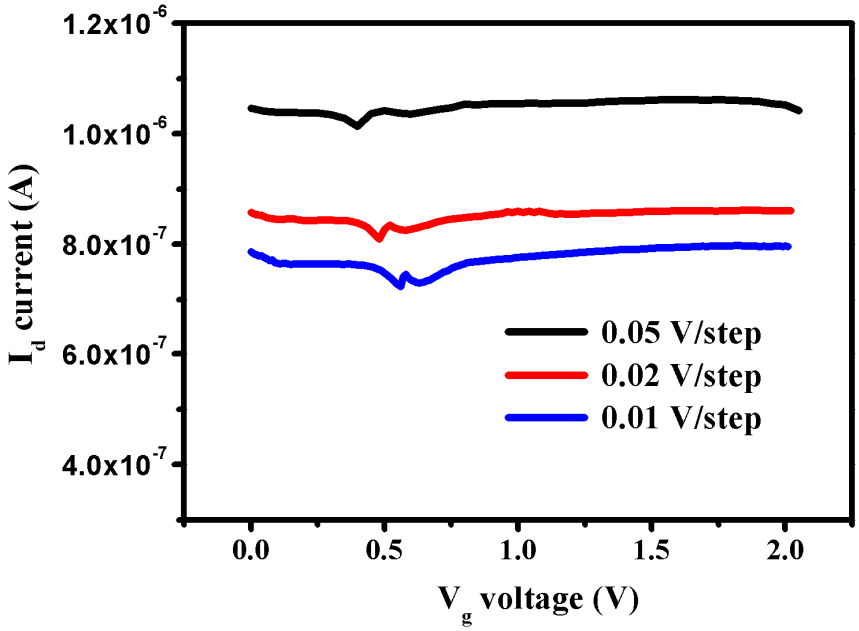

Figure S8. The I_d-V_g curve of the solution gate at different step voltages.

The I_d-V_g curves of both the back gate and the solution gate have been measured with the same step voltage in the electrolyte of 0.5 M H_2SO_4. It is found that the I_d-V_g curve of the solution gate changes little with the increasing of gate voltage, which can prove that the channel conductance hardly influenced by the solution gate. On the

other hand, the improvement of channel conductance accompany with the increasing of back gate is large and obviously higher than that from solution gate.

Furthermore, the I_d current of solution gate is larger than that of back gate. This result should be attributed from that the device acts as a capacitor while measure the I_d-V_g curve of solution gate, and a varied solution gate voltage is similar to a varied potential in capacitor to produce a capacitive current. In order to confirm that, we also measure the I_d-V_g curves of solution gate at different step voltages (lower step voltage has lower scan rate). The relevant results have been shown in the **Figure S8**, and verify our inference. In the actual catalytic test, the scan rate of measurement is largely slower than that of the measurement above, and the catalytic potential is also smaller than 1 V. So the solution gate hardly influence the electrochemical catalytic reaction.

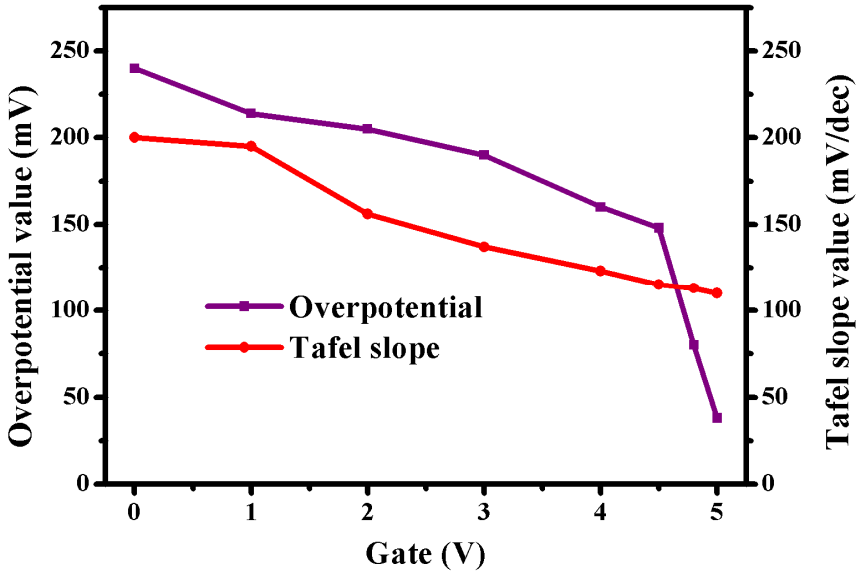

Figure S9. The variation curves of overpotential and Tafel slope with back gate voltages.

It can be found that the drop trends of overpotential and Tafel slope is similar and synchronous with the increasing of gate voltage from 0 to 4.5 V. Further increasing gate voltage, the tafel slope value decreases continuously while an inflection point appears at the gate voltage of 4.5 V for the overpotential value. We deduce that the dramatic drop of overpotential value comes from that the higher electric field can activate the active sites to reduce the Gibbs free energy of adsorbed atomic hydrogen. When the gate is increased to 4.5 V, the control of the charge transport to the overall catalytic reaction has reached to the limitation. This result in the Tafel value has arrived to 115 mV dec^{-1} at gate voltage of 4.5 V, which is almost same to the value of 116 mV dec^{-1} from the theory of Butler-Volmer. That means the control step of overall electrochemical catalytic reaction is transiting from only kinetic control to a mixture of the kinetic control and thermodynamic control. So the mediocre change of the channel conductance and Tafel slope value demonstrates that the large drop of the overpotential from the back gate voltage 4 V to 5 V can result from the improvement of activity of active site, not only the enhancement of charge transport.

Table S1. The overpotential at different gate voltages.

Gate (V)	0	1	2	3	4	4.5	4.8	5
Overpotential (mV)	240	214	205	190	160	148	80	38

Table S2. Tafel slope at different gate voltages.

Gate (V)	0	1	2	3	4	4.5	4.8	5
Tafel slope (mV/dec)	200	195	156	137	123	115	113	110

Table S3. Channel conductance of individual MoS_2 nanosheet based HER device at different gate voltages.

Gate (V)	-5	-4	-3	-2	-1	0
Conductance (S/m E-2)	0.73	0.99	1.46	2.10	3.06	5.50
Gate (V)	1	2	3	4	5	
Conductance (S/m E-2)	8.52	10.92	13.73	15.68	17.76	